# Investigation on the scan strategy and property of 316L stainless steel-Inconel 718 functionally graded materials fabricated by selective laser melting

Y. Zhou, X. Zhou, Q. Teng, Q.S. Wei, Y.S. Shi

State Key Laboratory of Die & Mould Technology, School of Materials Science and Engineering, Huazhong University of Science and Technology, Wuhan 430074, China

REVIEWED

## Abstract

316L stainless steel and Inconel 718 alloy functionally graded materials were fabricated by selective laser melting with a novel approach which combined powder-bed with powder-feed pattern. Two different scanning strategies have been used to form the steel/Ni FGMs. The interfacial characteristics were analyzed by scanning electron microscopy and energy dispersive spectroscopy. Quantitative evidence of good bonding at the interface was obtained from the tensile and shear tests of the steel/Ni FGMs.

## Introduction

Functional gradient materials (FGMs) have been concerned widely due to the important applications in corrosion-resistant and wear-resistant, electronic devices, coatings and thermal barrier coatings [1-3]. Recently, amount of researches focus on the forming process, gradient of structure or composition, microstructure and mechanical properties of the FGMs fabricated by additive manufacturing methods. For example, Ti-47Al-2.5V-Cr/Ti-6Al-2Zr-Mo-V gradient material was fabricated by the laser melting deposition (LMD) manufacturing process and the room-temperature tensile strength was up to approximately 1198.8 MPa [4]. In reference [5] Co-Cr-Mo material was deposited on a Ti-6Al-4V substrate transitioning from 0% to 100%. And it indicated that control over the cooling rate was a key to reduce the effects of thermal expansion differences between the two materials. However, there is little research on the interface between the two materials including the elements distribution, tensile and shear strength. Actually, it is very significant to make sure the interface characteristic which determines the whole property of the FGMs.

Due to the high corrosion resistance of the austenitic stainless steels and the excellent high-temperature property of the nickel-chromium alloy, the 316L stainless steel-Inconel 718 FGMs have been widely used in nuclear power generation and oil refineries [6]. Nevertheless, these two alloys are often still joined together by fusion welding, which can result in weak resistance to solidification cracking [7]. To overcome the cracking, selective laser melting (SLM) approach which is one of the additive manufacturing methods is chosen to form the steel/Ni FGMs.

This study firstly investigates the effect of scanning strategy on the densification

of the steel/Ni FGMs by the SLM process. Then the tensile and shear strength, elements distribution of the interface are characterized in order to fully understand the interface property of the steel/Ni FGMs.

## Materials and methods

### Materials

The spherical 316L stainless steel and Inconel 718 alloy powders prepared by gas atomization were used in this study. The powders have an average particle size 40 μm and 35 μm as shown in Fig.1, respectively.
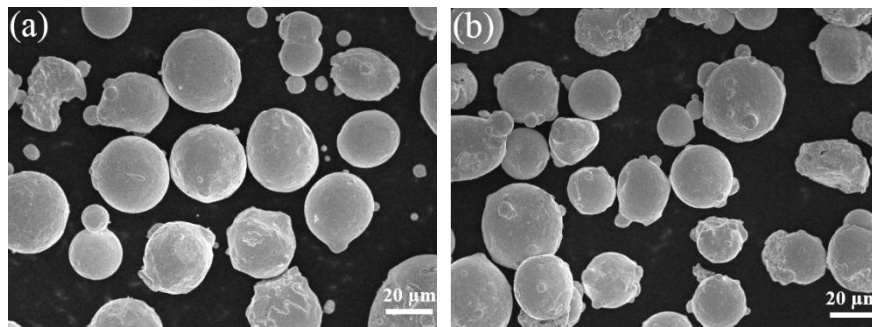


Fig. 1 SEM image shows the characteristic morphology of (a) 316L stainless steel powders and (b) Inconel 718 alloy powders.

### Machine and procedure

The HRPM-II SLM machine, developed by Huazhong University of Science and Technology, China, was employed to formed samples. This SLM machine is equipped with a continuous wave fiber laser, which processes a maximum laser output power of approximately 400 W and a wavelength of $1070 \pm 10$ nm. The spot size of the laser is about 100 μm, and the scanning speed can be adjusted from 50 to 1000 mm/s. The minimum thickness is 0.02 mm. Commercial 316L stainless steel plate with 10 mm thickness was used as the forming substrate plate. The building chamber of the SLM machine was vacuumized prior to the manufacturing processing, followed by filling of argon to form an anti-oxidating atmosphere. For the experiments of this paper, the following parameters were applied:
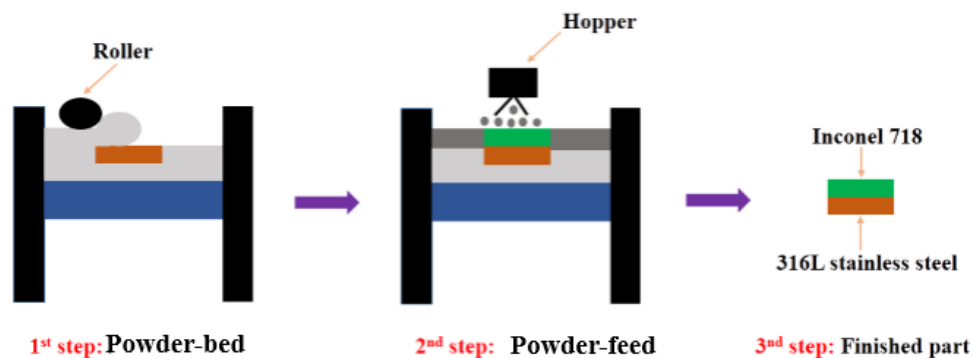


Fig. 2 Schematic diagram of the forming process of the FGMs by SLM.

- Laser beam power of 220 W.

- Laser scanning speed of 550 mm/s.
- Laser scanning spacing of 0.08 mm.
- Layer thickness of 0.02 mm.
- 316L stainless steel firstly formed with 1 mm in height by power-bed on the bottom and then Inconel 718 also formed with 1 mm in height by power-feed on the top as shown in Fig. 2.

**Analysis equipment and techniques**

The morphologies and microstructure of the samples were analyzed by optical microscope (OM, Shanghai) and (SEM, JSM-7600F, JEOL, Japan). The element variation was investigated by the energy dispersive spectroscopy (EDS) equipped on the SEM. The shearing strength test was carried out by the equipment developed by our team at room temperature. An Instron testing machine was used for tensile testing.

## Results and Discussion

**Influence of the scanning strategy**

A simulation results [8] show the antiparallel and parallel interlaced reverse scanning paths are found to be better than the other scanning strategies, such as in-spiral, out-spiral and Zigzag. The optimized scan strategy produced a high degree of thermal homogeneity while ensuring lower maximum temperature values. Given this, two alternative scanning strategies are selected (Fig. 3a and 3b). First one, it is called "line by line scanning strategy" (strategy A), with long bidirectional vectors. Another strategy, reducing the vector length by dividing the cross-section into islands is called "piece scanning strategy" (strategy B), scanned with short bidirectional vectors and changed $90^o$ for some interval. Samples with dimensions of $50 \times 10 \times 2$ mm (bottom 1mm for 316L, top 1 mm for Inconel) are produced for each scanning strategies, respectively.

The investigation first focuses on visual inspection and surface gloss to compare the quality factors such as delamination and porosity of the parts. The surface and side wall of the FGMs by different SLM strategies are obvious different (Fig. 3c-3f). It is easy to find that the poor surface gloss and apparent warping for strategy A (Fig. 3c), accompanied with the delamination between the two materials in the side wall. While, for strategy B (Fig. 3d), the samples exhibit excellent formability which the porosity has almost not been found and the interface of the side wall combined well (Fig. 3f).

According to the above results, it can be indicated that the laser is much more uniform due to the shorter scanning vector and the smaller scanning interval for piece scanning strategy than the line by line scanning strategy at the same forming parameters. Moreover, less energy is absorbed and heat is conducted away more quickly for long vector scanning. Due to the different properties of the 316L stainless steel and Inconel 718 at the interface, the shorter vector and smaller interval can reduce the difference step by step and obtain a good combination for these two materials. Therefore, the piece scanning strategy is beneficial to form the FGMs according to the performance.
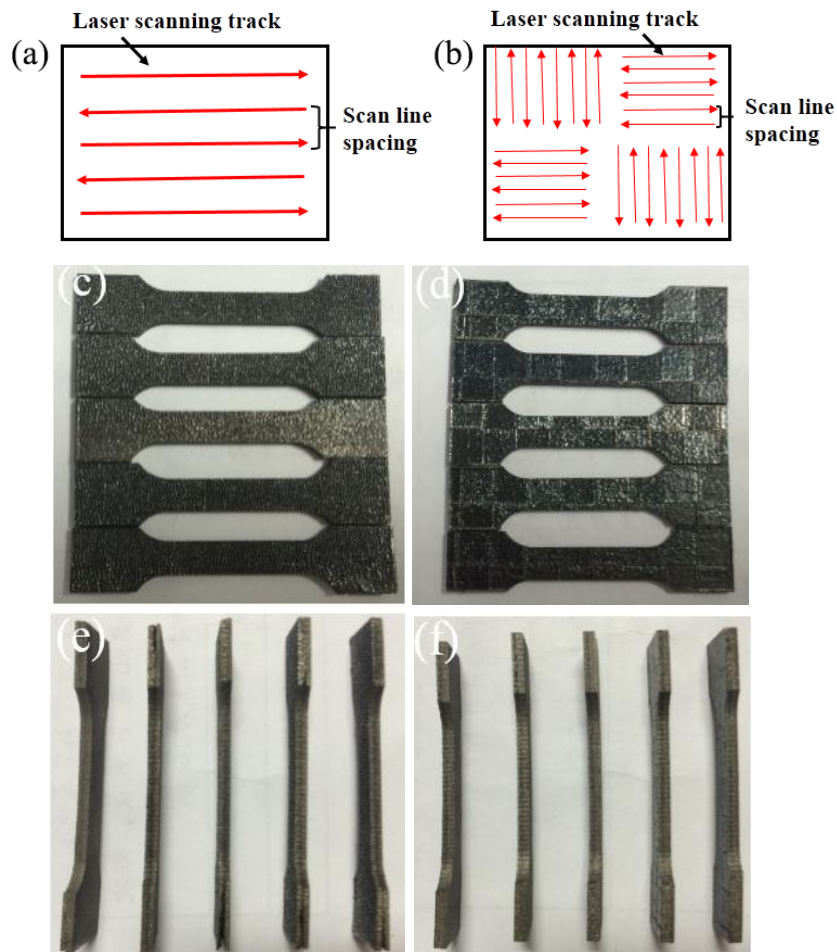
Fig. 3 The scanning strategy of (a) line by line scanning (b) piece scanning, the surface of real FGMs by (c) line by line scanning (d) piece scanning and the side wall (e) line by line scanning (f) piece scanning.

## Mechanical properties

Mechanical properties obtained from the tensile tests done on samples formed in two different scanning strategies A and B (as depicted in Fig. 3) are shown in Fig. 4. There are four available samples for strategy A (Fig. 4a) and five samples for strategy B (Fig. 4b). A first observation shows that the stress of samples with strategy B is much higher (720-800 MPa) than the samples with strategy A (200-650 MPa). Furthermore, the strain of samples with strategy B (6%-9%) appears bigger than strategy A (2%-7%) at the same time. The difference also can be explained by the formability for the two scanning strategies as depicted in Fig. 3.

Generally speaking, the tensile stress of 316L stainless steel formed by SLM is about 700 MPa, and the value of Inconel 718 is 680 MPa approximately. In this study, combining 316L stainless steel with the Inconel 718, the tensile stress of the FGMs is higher or at least comparable to the each material. From these results, it also can be concluded that there is good bonding at the interface for the steel/Ni FGMs.
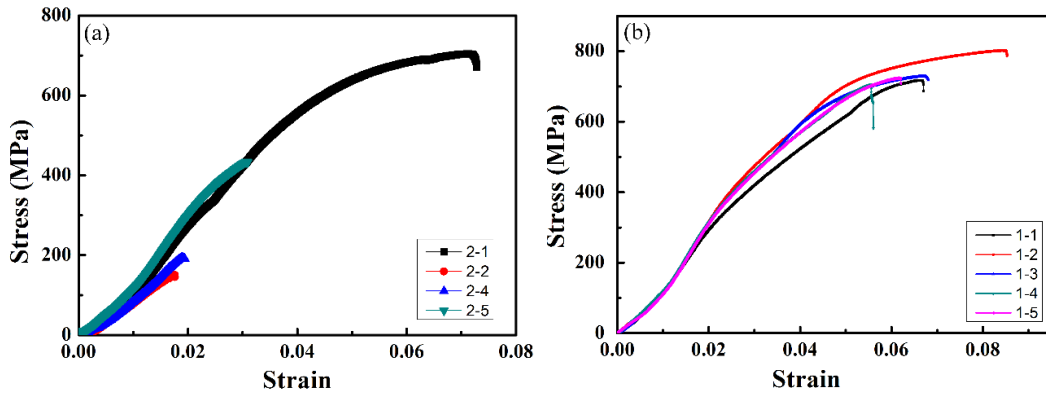
Fig. 4 The tensile stress-strain curve of steel/Ni FGMs formed by SLM with (a) line by line scanning (b) piece scanning.

Fig. 5 displays the tensile fracture surface of the samples formed in two different scanning strategies (as depicted in Fig. 3). It is worth noting that there are some spherical particles distributing in the fracture surface for both scanning strategies. Since the lower laser energy density for the long vector, the more spherical particles cannot be melted together for scanning strategy A as shown in Fig. 5a. In addition, it also can be indicated that the bonding of the two materials is so poor according to the obvious crack at the interface for scanning strategy A. However, there is not apparent crack at the interface and less spherical particles in the fracture surface for scanning strategy B in Fig. 5b. Therefore, the well bonding of the FGMs by SLM benefits from the shorter vector. The samples with shorter vector are tested in the subsequent experiment.

Besides, it can be confirmed their brittle cracking of the both samples from the fracture surface, which is accordance with the lower fracture strain (as depicted in Fig. 4). This is true for most material processed by SLM because the rapid cooling conditions always lead to a brittle phase. Therefore, in the aspect of the practical application of the material, it is necessary to apply thermal treatment for increasing ductility of the FGMs in the next stage of this work.
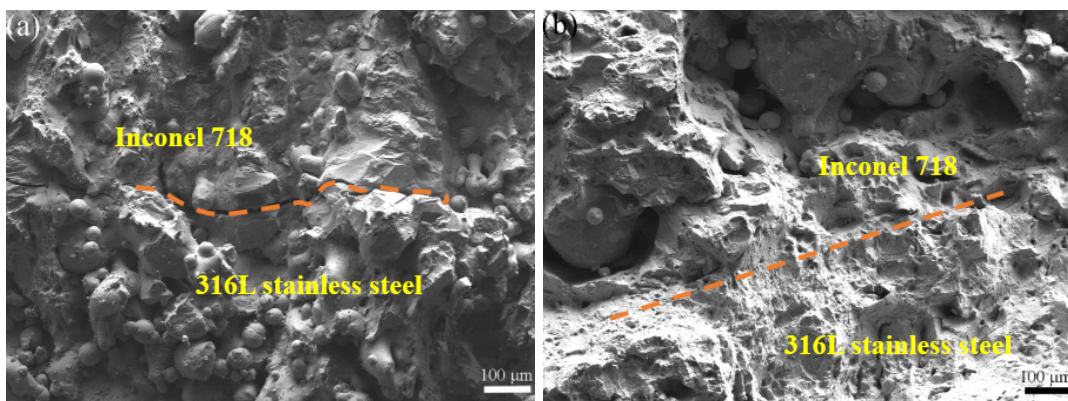


Fig. 5 The tensile fracture surface of 316L stainless steel-Inconel 718 FGMs formed by SLM with (a) line by line scanning (b) piece scanning.

The samples and devices for the shear stress test are exhibited in Fig. 6. The I-shape part is designed by ourselves which is made up of 45steel and the size can be adjusted according to the samples at some extent. The force is provided by hydraulic jack with digital readout to the side as shown in Fig. 6a. The samples used for the shear test include two segments, one is 316L stainless steel with dimensions of $20 \times 7 \times 1$ mm on the bottom and another is Inconel 718 with the same dimensions on the top. The area of overlap is $7 \times 7$ mm at the interface. Then a sample is plugged into the I-shape part and undergone the huge force from the hydraulic jack. At last, the data of the force can be written down when the sample breakup. All the samples are formed by the piece scanning strategy due to the good performance as displayed from Fig. 3 to Fig. 5.
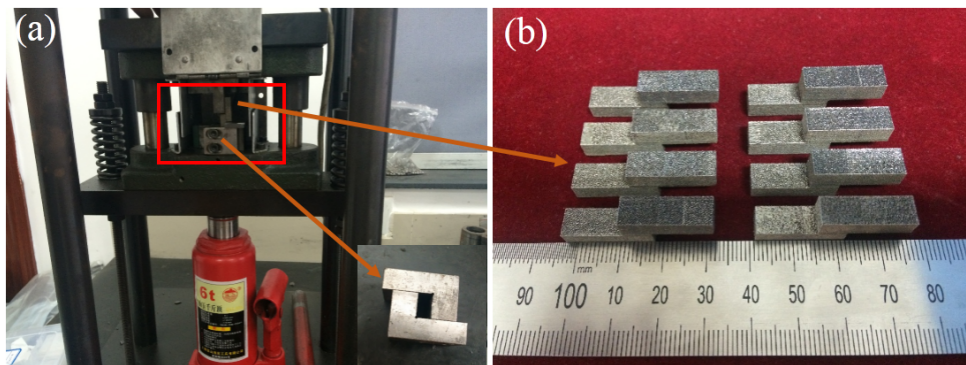


Fig. 6 The device of the shear stress test (a) and the samples (b) formed by SLM with the piece scanning.

Fig. 7 shows the shear stress of the samples formed by SLM with the piece scanning. It can be found that the shear strength varies from 516 MPa to 614 MPa. And the average value is about $581 \pm 11$ MPa, which is much higher than the cemented carbides-stainless steel (340 MPa) [9] and WC-carbon steel (370 MPa) [10] by brazing. The results are understandable, since the combination of the FGMs formed by SLM is metallurgical bond and it can reach up to a high shear stress.
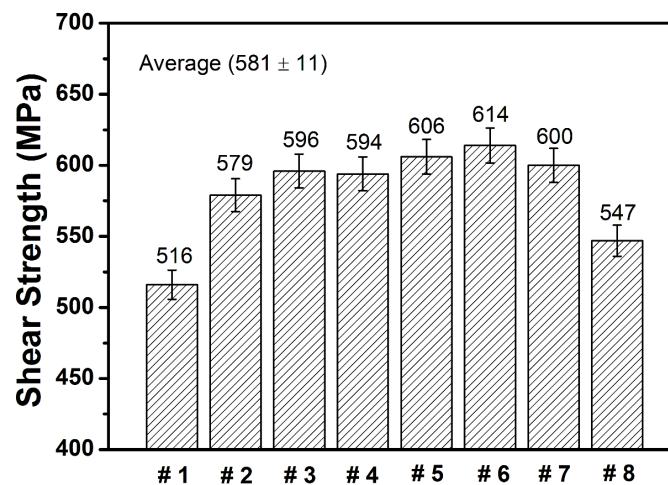


Fig. 7 The shear stress of the samples formed by SLM with the piece scanning.

**Interface**

The side wall of the steel/Ni interface with the piece scanning is displayed in Fig. 8. There are amount of un-melted balls on the surface and the interface cracking partly. Thus, process should be improved to obtain smooth side wall. Furthermore, the EDS mapping of the side wall of the steel/Ni interface is shown in Fig. 9. Due to the similar main elements (Fe, Ni, Cr), the element diffusion cannot be observed obviously at the bond interface. In the future, the line scanning of SEM will be carried out to make the element diffusion clearly.
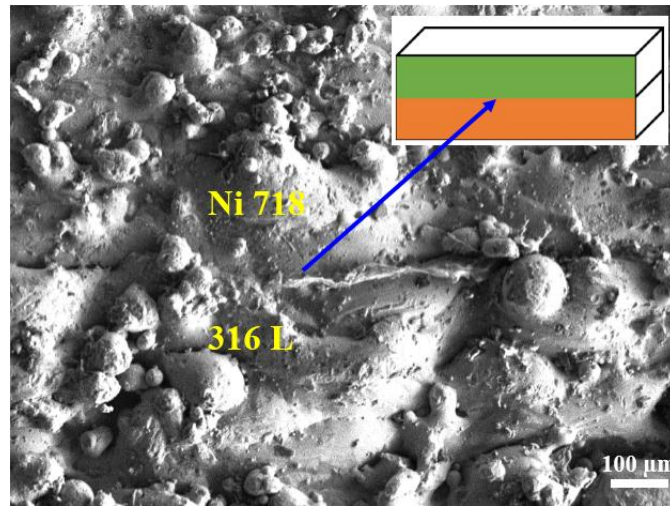


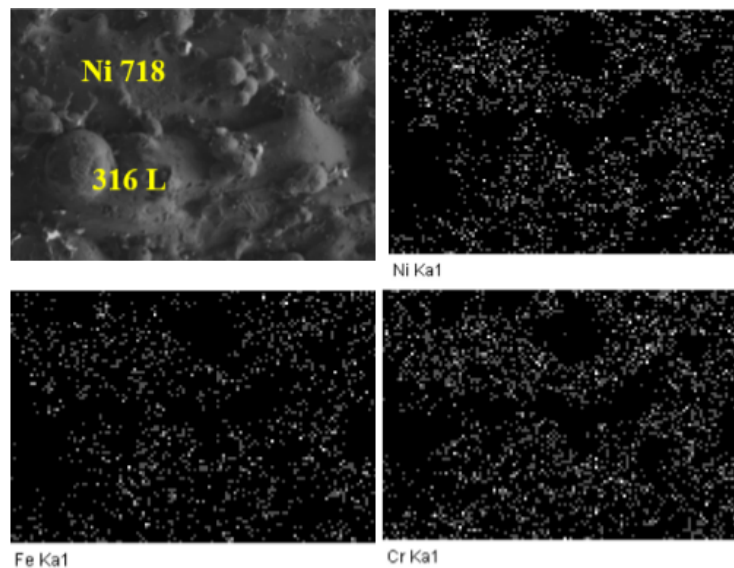Fig. 8 The side wall of the steel/Ni interface with the piece scanning.



Fig. 9 EDS mapping of the side wall of the steel/Ni interface.

**Conclusion**

- The piece scanning strategy is conducive to produced steel/Ni FGMs rather than the line by line scanning strategy due to the shorter scanning vector.
- The tensile and shear stress of steel/Ni FGMs formed by piece scanning strategy can reach up to 800MPa and 614 MPa, respectively.

- The ductility shows poor and the element diffusion at the interface exhibits not obviously at present. Therefore, process will be modified to improve the metallurgical bonding in the next step.

## References

[1] Gupta M, Loke CY. Synthesis of free standing, one dimensional, Al/SiC based functionally gradient materials using gradient slurry disintegration and deposition. Mater Sci Eng A 276, 2000, 210-217.

[2] Zhang YM, Han JC, Zhang XH, He XD, Li ZQ, Du SY. Rapid prototyping and combustion synthesis of TiC/Ni functionally gradient materials. Mater Sci Eng A 299, 2001, 218-524.

[3] Sakamoto N, Kawamura H. Preliminary characterization of interlayer for Be/Cu functionally gradient materials. J Nucl Mater 233, 1996, 609-611.

[4] H.P. Qu, P. Li, S.Q. Zhang, A. Li, H.M. Wang, Microstructure and mechanical property of laser melting deposition (LMD) Ti/TiAl structural gradient material, Materials and Design, 31,2010,574-582.

[5] J. M. Wilson, N. Jones, J. Li, Y. C. Shin, Laser deposited coatings of Co-Cr-Mo onto Ti-6Al-4V and SS316L substrates for biomedical applications, J Biomed Mater Res Part B 101B ,2013,1124-1132.

[6] K. Shah et al., Parametric study of development of Inconel-steel functionally graded materials by laser direct metal deposition, Materials and Design 54, 2014,531-538.

[7] J.L.Robinson, M.H. Scott, Liquation cracking during the welding of austenitic stainless steels and nickel alloys, Philos Trans R Soc London A (Math Phys Sci) 295,1980,105-17.

[8] S. Mohanty, C. C. Tutum, J. H. Hattel, Cellular scanning strategy for selective laser melting: Evolution of optimal grid-based scanning path & parametric approach to thermal homogeneity, Laser-based Micro- and Nanopackaging and Assembly VII, 8608,2013, 86080M-1.

[9] T.E. Yang, et al., Brazing behavior of ultrafine cemented carbide with stainless steel, J. Cent. South. Univ. 21, 2014, 2991-2999.

[10] W.B. Lee, Effects of Cr3C2 on the microstructure and mechanical properties of the brazed joints between WC-Co and carbon steel, International Journal of Refractory Metals & Hard Materials, 24, 2006, 215-221.